

The Catalytic Performance of MnSO₄-Doped Natural Zeolite in Ethyl Acetate Synthesis

Adelia Natasya Regita Nugroho^{a)}, Teguh Pambudi^{a*)}, Alfieta Rohmaful Aeni^{b)}, Retno Utami^{a)}

^{a)} Department of Chemical Engineering, Faculty of Engineering, Universitas Singaperbangsa Karawang, Karawang, 41361, Indonesia

^{b)} Department of Physics, Faculty of Engineering, Universitas Singaperbangsa Karawang, Karawang, 41361, Indonesia

^{*)} Corresponding Author: teguh.pambudi@ft.unsika.ac.id

Article history: received: 10-04-2025; revised: 09-06-2025; accepted: 06-07-2025; published: 06-07-2025

ABSTRACT

Ethyl acetate is a compound that is widely used across various industries. However, its esterification process typically requires a catalyst to improve reaction efficiency. This study focuses on developing a MnSO₄-doped natural zeolite catalyst using the impregnation method to enhance its catalytic activity in the esterification of acetic acid and ethanol. The synthesized catalyst was characterized using FTIR, XRD, and SEM-EDS to analyze structural and morphological changes. FTIR characterization revealed the presence of Si-O-Si and Al-O-Si bonds in the 1000 to 1100 cm⁻¹ region, while XRD confirmed that the zeolite with transition metal impregnation shows a decrease in the intensity of the diffraction peak. SEM-EDS analysis demonstrated that the MnSO₄-doped natural zeolite exhibited a more uniform morphology, with manganese ions effectively integrated into the surface and pores of the zeolite. Additionally, EDS measurements detected the presence of elements such as Si, O, Al, Na, and Mn, confirming the successful modification of the zeolite to act as a catalyst. Catalytic testing showed that the highest ethyl acetate conversion achieved was 91.27% within 90 minutes, with optimal performance observed at a catalyst mass of 1 g. These findings indicate that modifying zeolite with MnSO₄ can significantly enhance catalyst performance in esterification reactions, making it a more efficient and sustainable alternative to conventional catalysts.

Keywords: Catalyst, Zeolite, MnSO₄, Ethyl Acetate, Esterification

1. INTRODUCTION

Ethyl acetate is one of the most widely used materials in the solvent, flavoring, and fragrance industries [1]. Ethyl acetate is mainly produced through the esterification process between acetic acid and ethanol. The esterification reaction is typically carried out with a relatively long reaction time, so a catalyst is required to accelerate the process. In a study conducted [2] The esterification reaction between acetic acid and ethanol, without a catalyst, only produced low conversion within a specific time. Hence, the reaction that occurred was less effective in producing ethyl acetate.

The catalysts often used for the esterification of ethyl acetate are homogeneous mineral acid catalysts such as H₂SO₄, HCl, or H₃PO₄ [3]–[5]. However, the use of homogeneous acid catalysts has several

disadvantages. The catalyst is corrosive and toxic, which can cause potential environmental problems. In addition, separating homogeneous catalysts from their reactants and products is difficult [4], [6]. As a result, homogeneous catalysts tend to be less economically efficient because they can only be used once in one catalysis cycle.

Compared to homogeneous catalysts, heterogeneous catalysts offer advantages such as high selectivity, do not cause corrosion, can be recycled, and facilitate the easy separation of reactants and products [7]. Heterogeneous catalysts have a solid phase, so their separation is relatively simple because the particle size is larger than that of the liquid phase. The primary purpose of catalyst separation is to reuse the catalyst. Several types of solids that can be used as heterogeneous catalysts are metal oxides, zeolites,

clays, acid ion exchange resins, heteropolyacid salts, and metal-organic frameworks [8], [9].

Zeolite was chosen as the catalyst material in this study because it has several unique advantages that support its performance. This material is a crystalline aluminosilicate solid with a microporous structure, forming a three-dimensional network composed of tetrahedral units. The advantages of zeolite lie in its large surface area, thermal stability, and adjustable acidity and basicity. Zeolite catalysts have been used universally in various catalytic processes, such as biomass conversion, ethanol conversion, biofuel manufacturing, glycerol conversion, aromatic production, and various other products [10].

Additional treatment of the zeolite catalyst is needed to increase its activity in a catalysis process. The zeolite used as a catalyst must be activated before use. In natural zeolite, the acidification process is carried out to activate the zeolite by removing impurities that cover the pores of the zeolite framework. In this study, the material used for activation was sulfuric acid solution.

The physical and chemical properties of zeolite catalysts can also be improved by impregnating transition metals into the zeolite pores. Metals applied to zeolite through impregnation make zeolite a bifunctional catalyst, namely, the function of the metal and its carrier as a catalyst. The impregnated metal acts as a Lewis acid site, while the zeolite is active as a Bronsted acid [11]. Therefore, it is necessary to carry out transition metal impregnation to increase the effectiveness of zeolite as a catalyst.

Previous studies have mentioned that transition metals, such as Ni and Cu, can be loaded for the esterification process [12], [13]. Other studies also show that transition metals, such as Cr, Ni, and Pt, can be loaded on active natural zeolites through impregnation with good results. These metals show properties as catalytic activators in various reactions, such as the hydrogenation process of levulinic acid, CO₂ methanation, and carbohydrate conversion [14]–[16].

Transition metal impregnation has been shown to improve the catalytic efficiency of zeolite by providing additional active sites. In this study, MnSO₄ solution was added to activated zeolite to enhance its

catalytic performance in esterification. Manganese was selected due to its known catalytic activity and ability to increase the surface area of the zeolite, which facilitates faster reaction rates [12], [17].

2. METHODS

2.1. Materials and Instruments

A natural zeolite was obtained from Pudak Scientific. The zeolite has been ground to a size of 200 mesh. The chemicals, including sulfuric acid, NaOH, ethanol, manganese(II) sulfate monohydrate, oxalic acid dihydrate, and phenolphthalein indicator, were purchased from Merck. Acetic acid was obtained from Smartlab. All chemicals used were of analytical grade. For material characterization, a Fourier Transform Infrared (FTIR) spectrometer (Jasco 4000 series), an X-Ray Diffraction (XRD) diffractometer (Bruker D2-Phaser), and a Scanning Electron Microscopy (SEM) instrument (Hitachi SU-3500 brand) were utilized.

2.2. Experiment.

2.2.1. Zeolite Activation

Zeolite is activated using 4N sulfuric acid in a ratio of zeolite to an acid solution of 1:10. Furthermore, activation is carried out at 98°C for 2 hours. After the activation process, the activated zeolite is washed with distilled water until it reaches a neutral pH, and then it is drained to remove excess water from the pores of the zeolite. Zeolite is dried in an oven at a temperature of 105°C for 2 hours. Activated zeolite must be neutralized to avoid ethanol reacting with sulfuric acid and producing monosulfate. This condition will cause a decrease in ethanol-acetic acid contact and affect the conversion of acetic acid produced [18]. This stage produces activated zeolite catalysts. This catalyst is then utilized in the esterification process and further characterized using FTIR, XRD, and SEM techniques. This activation procedure refers to the methods that have been carried out [2], [18], [19].

2.2.2. Wet Impregnation of Mn on Zeolite

In the first stage, 20 g of activated zeolite was mixed with 100 mL of MnSO₄ metal solution, where the amount of Mn metal was 5% of the zeolite [12]. The mixture was then refluxed for 2 hours at 90 °C. After reflux, the zeolite mixture was filtered. The solids from

this process were then dried in an oven at 100 °C until dry. Furthermore, the solids were calcined at 550 °C for 4 hours. After the calcination process, the solids were ground and sieved to a size of 200 mesh. At this stage, MnSO₄-doped natural zeolite catalysts were produced. This catalyst was then utilized in the esterification process and subsequently characterized using FTIR, XRD, and SEM techniques.

2.2.3. Esterification of Ethyl Acetate

In the esterification process, ethanol and acetic acid are mixed in a reactor, specifically an Erlenmeyer flask, in a 1:1 ratio. Next, a catalyst is introduced into the reactor, and the mixture is heated to a temperature of 70 °C [18]. This process is carried out with variations in reaction time and different amounts of catalyst to examine their effects on conversion results. After reaching the designated temperature, the mixture is allowed to react for a specified time. The study focuses on the impact of different catalyst amounts on the conversion of acetic acid. The amounts of catalyst tested were 0 g, 0.25 g, 0.5 g, 1 g, 1.5 g, and 2 g. Samples were collected at intervals of 0, 15, 30, 60, 90, and 120 minutes after the reaction commenced. For comparison, esterification was also conducted without a catalyst.

2.2.4. Conversion Calculation

The collected samples are analyzed to determine the initial concentration (A_o) and the final concentration (A_s) of acetic acid through acid-base titration using 1 N NaOH, which has previously been standardized using oxalic acid [18]. The amount of acetic acid converted into products can be calculated using equation (1):

$$x_A = \frac{A_o - A_s}{A_o} \times 100\% \quad (1)$$

while x_A = acetic acid conversion

3. RESULTS AND DISCUSSION

3.1. Fourier Transform Infrared (FTIR)

The zeolite samples exhibit peaks in the wavenumber range of 1000–1100 cm⁻¹, which are typically related to the Si-O-Si and Al-O-Si vibrations in the TO₄ tetrahedra (where T = Si or Al) [20]. The

spectrum of activated zeolites shows a higher frequency compared to untreated pure zeolites. Specifically, there is a shift in the absorption band from 1009 cm⁻¹ in pure zeolite to 1011 cm⁻¹ in the activated zeolite. This shift aligns with previous studies [21], [22], which indicates that the dealumination process reduces the number of Al atoms in the zeolite framework. This reduction decreases the Al-O-Si interaction, leading to an increase in the Si-O-Si vibration frequency. When pure natural zeolite is treated with acid, dealumination occurs as a structural modification of the framework. This process may also be accompanied by the removal of exchangeable cations and other impurities, which can otherwise block the zeolite's pores.

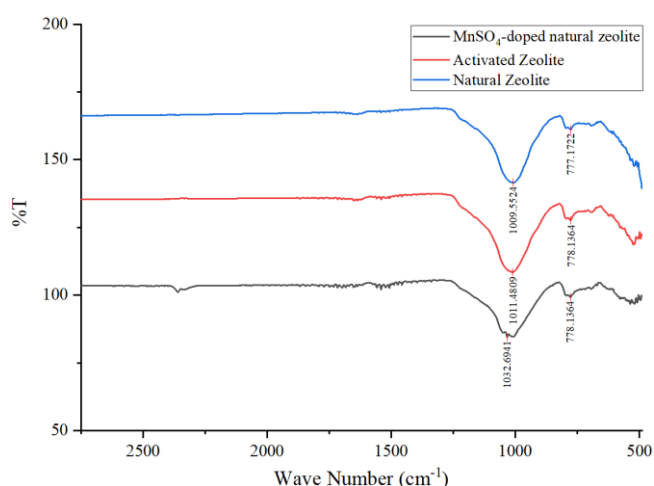


Figure 1. FTIR spectra of pure zeolite, activated zeolite, and MnSO₄-doped natural zeolite.

Additionally, the FTIR spectrum indicates a reduction in impurity levels. Interfering chemicals are eliminated, and the exchangeable sites are rearranged by chemical activation [23]. MnSO₄-doped natural zeolite exhibited a band shift from activated zeolite to 1032 cm⁻¹, exhibiting the same phenomenon. The band shift is likely due to structural changes in the zeolite framework caused by the interaction between Mn²⁺ ions and the Si-O/Al-O bonds. This interaction may alter the bond strength and geometry, leading to a shift in the symmetric stretching vibration frequency

The zeolite exhibits symmetric stretching vibrations of O-Si-O/O-Al-O in the wavenumber range of 650-820 cm⁻¹, with a peak at around 794 cm⁻¹ [24]. Thus, the bands at 777 and 778 cm⁻¹ are most likely due

to the external symmetric stretching vibrations and internal tetrahedra in the zeolite structure [25].

3.2. X-Ray Diffraction (XRD)

Changes in X-ray diffraction values on activated zeolite and after impregnation with Mn metal are shown in Figure 2. The graph shows a prominent peak between 26° and 29° , which indicates that clinoptilolite and mordenite phases were observed [26]. The sharpness of this diffraction peak suggests that the resulting zeolite possesses desirable crystallinity, a property that is generally essential for applications such as catalysts or adsorbents [27].

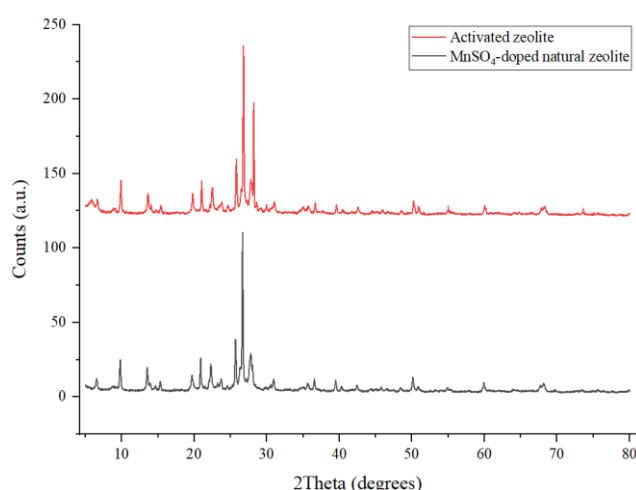


Figure 2. X-ray diffraction patterns of activated zeolite catalyst samples and MnSO_4 -doped natural zeolite.

The crystallinity area is described as having a narrow and sharp peak, while the area with a widened peak is amorphous. Based on [22], zeolite with transition metal impregnation shows a decrease in the intensity of the diffraction peak, this indicates that the metal is not only attached to the surface of the zeolite, but the metal has entered the zeolite structure, so that there is a decrease in the intensity of the crystallinity and the dominant amorphous region that appears. Changes in the intensity and peak of the crystallinity region occur because the zeolite, which was previously in the form of pores filled with cations, is replaced by metal elements. This replacement causes a significant change in the angles of incidence of an X-ray, which varies with the presence of transition metals adsorbed and replacing the cations in the initial zeolite. This

change will affect the angle of crystal scattering, so that the intensity and peak will decrease or change [28].

Similar results were obtained in this study with MnSO_4 doping. MnSO_4 -doped natural zeolites also retain most of the zeolite diffraction patterns, but with specific changes. The shift in peak positions or changes in intensity may indicate interactions between Mn ions and the zeolite structure, either through ion substitution or the formation of new phases. Mn^{2+} can enter the pores and channels of the zeolite through the impregnation process and can replace cations in the zeolite structure, such as Na^+ , K^+ , or Ca^{2+} . The most likely ion to be replaced by Mn^{2+} in the zeolite structure is Ca^{2+} , because both have the same charge (+2) and relatively close ion sizes. In ion exchange, the compatibility of charge and ion size is a key factor that determines the possibility of substitution in the zeolite framework. This substitution can change the distance between crystallographic planes in the zeolite, causing some XRD peaks to shift or even disappear.

Thus, the zeolite framework was successfully maintained despite the introduction of transition metals. However, a reduction in the percentage of crystallinity was noted with the transition metal modification [17].

3.3. Scanning Electron Microscopy (SEM)

The SEM images of the MnSO_4 metal-doped natural zeolite and the activated zeolite catalyst sample are illustrated in Figure 3. After impregnation, the crystal morphology did not show any significant changes [29]. In addition, the Si/Al ratio did not change during the impregnation process, which is further evidence that the impregnation process did not affect the overall composition of the zeolite framework [17], [29].

According to Figures 3a and 3b, the activated zeolite demonstrated particles that were comparatively rough and had non-uniform diameters [30]. The activation process removes impurities or undesirable elements to enhance the surface area and create active sites. The development of active sites on the surface is indicated by the apparent opening of the pore structure without any impurities [31]. The comparatively rough appearance of the particle surface suggests that the activation process has changed the texture.

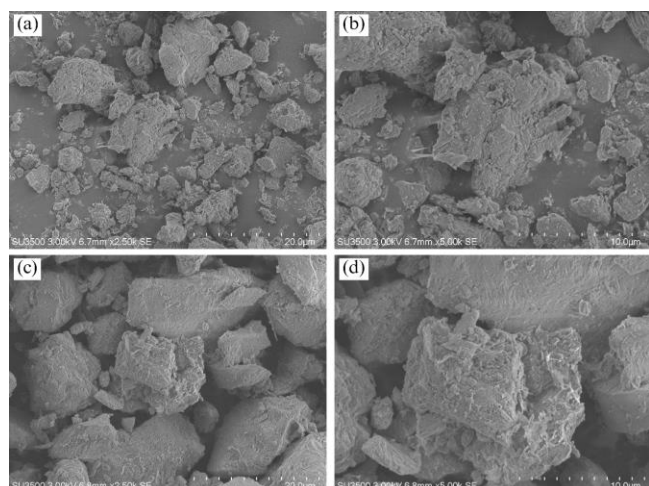


Figure 3. Morphology of natural zeolite samples: (a) activated at 2,500x magnification, (b) activated at 5,000x magnification, (c) MnSO₄-doped at 2,500x magnification, (d) MnSO₄-doped at 5,000x magnification.

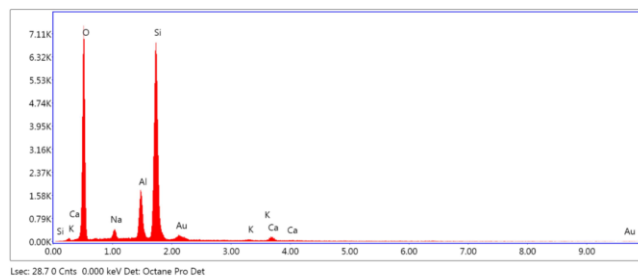
The morphology of the MnSO₄-doped natural zeolite shows particles that look larger and more uniform than the activated zeolite (Figures 3c and 3d). MnSO₄-doped natural zeolite shows particles that look larger and more uniform than the activated zeolite, which may be attributed to the successful dispersion of Mn²⁺ ions that promote crystal growth and reduce surface defects during the impregnation process. In the MnSO₄-doped natural zeolite, metal ions are seen to be clustered together, resulting in more obvious changes in surface morphology [17]. The appearance of MnSO₄-doped natural zeolite shows an indication of the formation of a crystal area in the form of dispersed white lumps, and metal appears to be attached to the surface of the zeolite. This shows that the impregnation treatment has gone well [32]. The even dispersion of Mn is expected to increase the surface area [22].

The results of the EDS analysis for MnSO₄-doped natural zeolite samples are presented in Figure 4 and Table 1. Based on the EDS results, the activated zeolite contains the main elements Si, O, Al, and Na. MnSO₄-doped natural zeolite also has the same main composition as the doped zeolite after the impregnation process, which confirms that the impregnation process does not affect the overall composition of the zeolite framework [29]. This is consistent with the basic structure of the zeolite after the modification process,

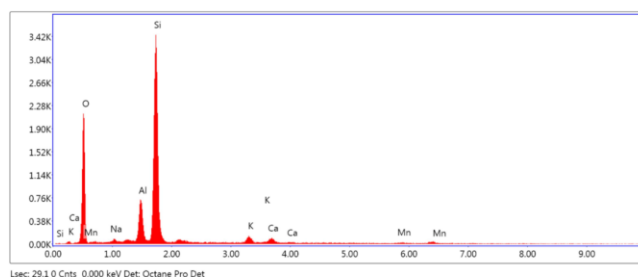
because these elements are the main components of the zeolite framework. In addition, the EDS spectrum of MnSO₄-doped natural zeolite also indicates the presence of a new compound, namely Mn. This shows that the Mn metal from MnSO₄ was successfully attached to the zeolite through the impregnation process.

Table 1. Elemental content in activated zeolite and metal-doped zeolite

Activated Zeolite		MnSO ₄ -doped natural zeolite	
Element	Composition (%) by weight	Element	Composition (%) by weight
O	51.08	O	52.03
Na	1.90	Na	1.70
Al	7.63	Al	7.36
Si	33.40	Si	34.31
Au	2.68	K	1.09
K	1.72	Ca	1.49
Ca	1.59	Mn	2.02



(a)



(b)

Figure 4. EDS spectra of (a) activated, (b) MnSO₄-doped natural zeolite samples.

3.4. Effect of Reaction Time on Acetic Acid Conversion

In this study, the variation of reaction time used to determine the optimum reaction time was at 0, 15, 30, 60, 90, and 120 minutes. The effect of reaction time on the esterification of acetic acid with ethyl alcohol was investigated using three different methods: without

a catalyst, with an activated zeolite catalyst, and with MnSO₄-doped natural zeolite. The experiments were conducted at a temperature of 70 °C, with a reactant molar ratio of 1:1, and a catalyst mass of 1 g.

Figure 5 shows the conversion of acetic acid with the effect of reaction time. In the blank sample, the acetic acid conversion ranged from 87.79% to 88.61% over the entire time. This indicates that the reaction without a catalyst is slower and the conversion is lower. The curve shows a relatively flat trend with a slight increase in conversion over time.

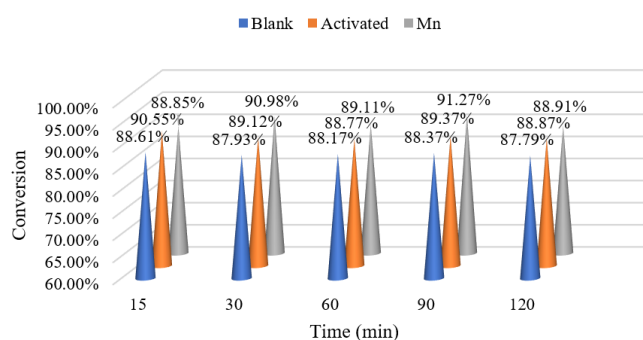


Figure 5. Effect of reaction time on acetic acid conversion (%).

In the activated zeolite sample, the conversion value ranged from 88.87% to 90.54%, indicating that the increase in conversion was more significant compared to the blank. This suggests that the increase in catalytic activity in activated zeolite accelerates the conversion process of acetic acid to ethyl acetate. This is because the activation process has opened the pores of the zeolite and expanded its surface area, thereby increasing the number of active sites exposed to react.

The MnSO₄-doped natural zeolite sample has the highest conversion rate, ranging from 88.85% to 91.27% after 120 minutes. The catalytic activity of MnSO₄-doped natural zeolite shows a slight enhancement, so that the reaction proceeds faster and the conversion is higher than that of the blank and activated zeolite catalyst.

The maximum conversion of acetic acid, 91.27%, was obtained at an esterification time of 90 minutes using a MnSO₄-doped natural zeolite catalyst. At a reaction time of 15 minutes, the conversion of acetic acid was relatively the same for all samples. Still, at 30-120 minutes, the conversion increased more sharply in the activated and Mn samples.

Catalysts play a crucial role in enhancing the reaction rate, thereby increasing efficiency and selectivity. However, the relationship between catalyst concentration and reaction rate is complex and can vary, depending on the nature of the catalyst and the specific organic reaction involved [33]. Although there was a fluctuation in this study, it can occur because the esterification reaction is reversible. Therefore, the longer the reaction time, the more likely the products formed are to revert to the reactants.

3.5. Effect of Added Catalyst Mass (Catalyst Loading)

The effect of catalyst loading was investigated using an activated zeolite catalyst and a MnSO₄-doped natural zeolite, both at a temperature of 70 °C and a 1:1 molar ratio of reactants, for 30 minutes. The variations of the catalyst added were 0, 0.25, 0.50, 1.00, 1.50, and 2.00 g.

Figure 6 presents a graph of the results of acetic acid conversion, illustrating the relationship between catalyst loading and conversion percentage. In the graph, there is a fluctuation in the conversion of acetic acid along with the addition of the catalyst mass. This fluctuation is evident in the inconsistent changes in conversion values. The maximum conversion of acetic acid was recorded at 90.98% in 1 g of MnSO₄-doped natural zeolite. At a catalyst mass of 0 g, both catalysts showed a conversion of 87.93%. This indicates that the reaction can still occur even without a catalyst, although the conversion value is relatively low and can still be improved.

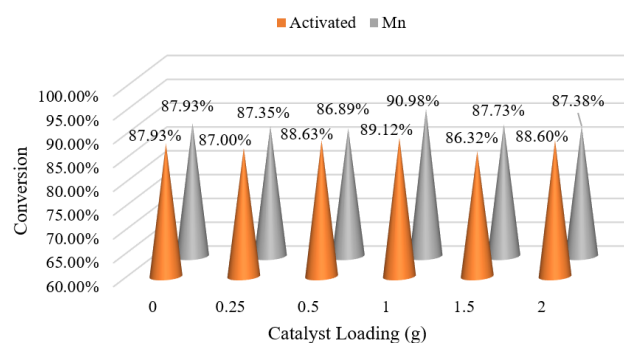


Figure 6. Effect of catalyst loading on acetic acid conversion (%).

When the catalyst mass was increased to 0.25 g, the increase in conversion for the activated zeolite

catalyst was not significant, at 87.00%. In contrast, for the MnSO₄-doped natural zeolite catalyst, the increase was more critical, with a value of 87.34%. This indicates that the activated zeolite catalyst is more efficient in accelerating the reaction.

When the catalyst mass was 0.5 g, there was a decrease in the conversion of acetic acid in both types of catalysts. The MnSO₄-doped natural zeolite catalyst gave better conversion results than the activated zeolite, which was 88.63% for MnSO₄-doped natural zeolite and 86.89% for activated zeolite. This shows that MnSO₄-doped natural zeolite shows a positive effect on higher acetic acid conversion compared to activated zeolite. However, there is a decrease in conversion compared to the addition of 0.25 g of catalyst.

At a catalyst mass of 1 g, the conversion for both catalysts reached the highest level, with a conversion value of 90.98% for MnSO₄-doped natural zeolite and 89.12% for activated zeolite. This indicates that, at this point, both catalysts are effective; however, MnSO₄-doped natural zeolite remains superior in increasing conversion.

At catalyst masses of 1.5 and 2 g, a decrease in conversion was observed for both types of catalysts. At 1.5 g, the conversion reached 87.72% for MnSO₄-doped natural zeolite and 86.32% for activated zeolite. Meanwhile, at 2 g, the conversion was recorded at 88.60% for activated zeolite and 87.38% for MnSO₄-doped natural zeolite. This decrease is thought to be due to catalyst saturation, where the addition of more catalyst mass no longer increases the reaction efficiency; thus, the catalyst, which should function to improve the activation reaction rate, stops its activity.

4. CONCLUSION

The study demonstrates that MnSO₄-doped natural zeolite enhances catalytic performance in the esterification of acetic acid and ethanol to produce ethyl acetate. Analyses using FTIR, XRD, and SEM-EDS confirmed the successful modification of the zeolite, showing that Mn ions are well-dispersed within its structure. Catalytic tests revealed an impressive acetic acid conversion rate of 91.27% within 90 minutes when using 1 g of MnSO₄-doped natural zeolite. However, increasing the catalyst mass beyond

this point reduced efficiency due to saturation effects. MnSO₄-doped natural zeolite is a sustainable and efficient heterogeneous catalyst suitable for various esterification and catalytic processes.

REFERENCES

- [1] Z. Felfelian and M. Mahdavi, "A new ZrC nano powder solid acid catalyst for the esterification synthesis of ethyl acetate," *Catal. Commun.*, vol. 182, no. August, p. 106752, 2023, doi: 10.1016/j.catcom.2023.106752.
- [2] C. C. S. Nindya, D. R. Anggara, Nuryoto, and K. Teguh, "Esterification glycerol (by product in biodiesel production) with oleic acid using mordenite natural zeolite as catalyst: Study of reaction temperature and catalyst loading effect," *IOP Conf. Ser. Mater. Sci. Eng.*, vol. 909, no. 1, 2020, doi: 10.1088/1757-899X/909/1/012001.
- [3] J. Ma, S. Wang, Y. Duan, C. Ding, and X. Wang, "Synthesis of Ethyl Acetate by the Esterification Process: Process Optimization," *Eng. Adv.*, vol. 3, no. 6, pp. 449–453, 2024, doi: 10.26855/ea.2023.12.002.
- [4] P. Sahu and A. Sakthivel, "Zeolite-β based molecular sieves: A potential catalyst for esterification of biomass derived model compound levulinic acid," *Mater. Sci. Energy Technol.*, vol. 4, pp. 307–316, 2021, doi: 10.1016/j.mset.2021.08.007.
- [5] F. Yang and J. Tang, "Catalytic Upgrading of Renewable Levulinic Acid to Levulinate Esters Using Perchloric Acid Decorated Nanoporous Silica Gels," *ChemistrySelect*, vol. 4, no. 4, pp. 1403–1409, 2019, doi: 10.1002/slct.201803608.
- [6] Q. Zhang *et al.*, "Environmentally-friendly preparation of Sn(II)-BDC supported heteropolyacid as a stable and highly efficient catalyst for esterification reaction," *J. Saudi Chem. Soc.*, vol. 28, no. 3, p. 101832, 2024, doi: 10.1016/j.jscs.2024.101832.
- [7] B. M. Kurji and A. S. Abbas, "MCM-48 from rice husk ash as a novel heterogeneous catalyst for esterification of glycerol with oleic acid: Catalyst preparation, characterization, and activity," *Case Stud. Chem. Environ. Eng.*, vol. 8, no. May, p. 100382, 2023, doi: 10.1016/j.csce.2023.100382.
- [8] A. Kokel, C. Schäfer, and B. Török, "Organic Synthesis Using Environmentally Benign Acid Catalysis," *Curr. Org. Synth.*, vol. 16, no. 4,

- pp. 615–649, 2019, doi:
10.2174/1570179416666190206141028.
- [9] R. Yahya and R. F. M. Elshaarawy, “Highly sulfonated chitosan-polyethersulfone mixed matrix membrane as an effective catalytic reactor for esterification of acetic acid,” *Catal. Commun.*, vol. 173, p. 106557, 2023, doi: 10.1016/j.catcom.2022.106557.
- [10] A. Rafiani, D. Aulia, and G. T. M. Kadja, “Zeolite-encapsulated catalyst for the biomass conversion: Recent and upcoming advancements,” *Case Stud. Chem. Environ. Eng.*, vol. 9, p. 100717, 2024, doi: 10.1016/j.csee.2024.100717.
- [11] S. Sumari, F. Fajaroh, I. Bagus Suryadharma, A. Santoso, and A. Budianto, “Zeolite Impregnated with Ag as Catalysts for Glycerol Conversion to Ethanol Assisted by Ultrasonic,” *IOP Conf. Ser. Mater. Sci. Eng.*, vol. 515, no. 1, 2019, doi: 10.1088/1757-899X/515/1/012075.
- [12] O. C. H. Arjek and I. Fatimah, “Modifikasi Zeolit Dengan Tembaga (Cu) Dan Uji Sifat Katalitiknya Pada Reaksi Esterifikasi,” *Chemical*, vol. 3, no. 1, pp. 20–27, 2017, doi: 10.20885/ijcr.vol2.iss1.art3.
- [13] W. Trisunaryanti, E. Triwahyuni, and S. Sudiono, “PREPARATION, CHARACTERIZATIONS AND MODIFICATION OF Ni-Pd/NATURAL ZEOLITE CATALYSTS,” *Indones. J. Chem.*, vol. 5, no. 1, pp. 48–53, 2005, doi: 10.22146/ijc.21838.
- [14] A. Al-khawlani *et al.*, “Enhanced catalytic activity and high stability of treated Pt-Ru/zeolite Y catalysts for levulinic acid hydrogenation reaction,” *Catal. Commun.*, vol. 183, 2023, doi: 10.1016/j.catcom.2023.106761.
- [15] D. Spataru *et al.*, “International Journal of Hydrogen Energy Doping Ni / USY zeolite catalysts with transition metals for CO₂ methanation,” vol. 53, no. October 2023, pp. 468–481, 2024, doi: 10.1016/j.ijhydene.2023.12.045.
- [16] S. Xu *et al.*, “Highly efficient Cr/B zeolite catalyst for conversion of carbohydrates into 5-hydroxymethylfurfural: Characterization and performance,” *Fuel Process. Technol.*, vol. 190, pp. 38–46, 2019, doi: 10.1016/j.fuproc.2019.03.012.
- [17] I. M. S. Anekwe, B. Oboirien, and Y. M. Isa, “Effects of transition metal doping on the properties and catalytic performance of ZSM-5 zeolite catalyst on ethanol-to-hydrocarbons conversion,” *Fuel Commun.*, vol. 18, no. December, p. 100101, 2024, doi: 10.1016/j.fueco.2023.100101.
- [18] Nuryoto, A. R. Amaliah, A. Puspitasari, and A. D. Ramadhan, “Study of Esterification Reaction Between Ethanol and Acetic Acid Using Homogeneous and Heterogeneous Catalyst,” *World Chem. Eng. J.*, vol. 4, no. 2, p. 51, 2020, doi: 10.48181/wcej.v4i2.8952.
- [19] Nuryoto, H. Sulisty, W. B. Sediawan, and I. Perdana, “Modifikasi Zeolit Alam Mordenit Sebagai Katalisator Katalisasi dan Esterifikasi,” *Reaktor*, vol. 16, no. 2, pp. 72–80, 2016.
- [20] T. Nasution, A. M. Pulungan, Y. A. Wiliranti, J. L. Sihombing, and A. N. Pulungan, “Synthesis of Biodiesel From Rubber Seed Oil with Acid and Base Activated Natural Zeolite Catalyst,” *Indones. J. Chem. Sci. Technology*, vol. 02, no. 2, pp. 125–130, 2019.
- [21] C. A. Susiana, B. Rusdiarso, and M. Mudasir, “Enhanced Capacity and Easily Separable Adsorbent of Dithizone-immobilized Magnetite Zeolite for Pb(II) Adsorption,” *Indones. J. Chem.*, vol. 24, no. 4, pp. 1058–1070, 2024, doi: 10.22146/ijc.90914.
- [22] R. N. Yanti, E. Hambali, G. Pari, and A. Suryani, “Analisis Karakteristik Fungsi Zeolit Alam Aktif Sebagai Katalis Setelah Diimpregnasi Logam Nikel,” *J. Penelit. Has. Hutan*, vol. 39, no. 3, pp. 138–147, 2021, doi: 10.20886/jphh.2021.39.3.138-147.
- [23] P. D. Anghistra, Pardoyo, and A. Subagio, “Modifikasi Zeolit Alam dengan Mn pada Pengaruh Asam dan High Energy Milling,” *Greensph. J. Environ. Chem. Orig.*, vol. 3, no. 2, pp. 1–5, 2023.
- [24] M. Faisal, Suhartana, and Pardoyo, “Zeolit Alam Termodifikasi Logam Fe sebagai Adsorben Fosfat (PO₄ 3-) pada Air Limbah,” *J. Kim. Sains dan Apl.*, vol. 18, no. 3, pp. 91–95, 2015.
- [25] H. Aloulou, H. Bouhamed, A. Ghorbel, R. Ben Amar, and S. Khemakhem, “Elaboration and characterization of ceramic microfiltration membranes from natural zeolite: Application to the treatment of cuttlefish effluents,” *Desalin. Water Treat.*, vol. 95, no. August, pp. 9–17, 2017, doi: 10.5004/dwt.2017.21348.
- [26] A. Mustain, G. Wibawa, M. F. Nais, and M. Falah, “Synthesis of Zeolite NaA from Low

- Grade (High Impurities) Indonesian Natural Zeolite,” *Indones. J. Chem.*, vol. 14, no. 2, pp. 138–142, 2014, doi: 10.22146/ijc.21250.
- [27] M. Ali, “Qualitative analyses of thin film-based materials validating new structures of atoms,” *Mater. Today Commun.*, vol. 36, no. May, 2023, doi: 10.1016/j.mtcomm.2023.106552.
- [28] F. W. Chang, M. S. Kuo, M. T. Tsay, and M. C. Hsieh, “Hydrogenation of CO₂ over nickel catalysts on rice husk ash-alumina prepared by incipient wetness impregnation,” *Appl. Catal. A Gen.*, vol. 247, no. 2, pp. 309–320, 2003, doi: 10.1016/S0926-860X(03)00181-9.
- [29] S. Hajimirzaee, A. Soleimani Mehr, and E. Kianfar, “Modified ZSM-5 Zeolite for Conversion of LPG to Aromatics,” *Polycycl. Aromat. Compd.*, vol. 42, no. 5, pp. 2334–2347, 2020, doi: 10.1080/10406638.2020.1833048.
- [30] P. Pardoyo, Y. Astuti, G. Herinnayah, S. Suhartana, and P. J. Wibawa, “The influence of high energy milling to the adsorption of Cd(II) and Zn(II) ions on activated zeolite,” *J. Phys. Conf. Ser.*, vol. 1524, no. 1, 2020, doi: 10.1088/1742-6596/1524/1/012080.
- [31] F. Fadliah, C. Palit, R. Pratiwi, R. Aryanto, and T. W. Putri, “Analysis the Effect of Activated Natural Zeolites for Fe Metal Adsorption,” *Walisongo J. Chem.*, vol. 6, no. 2, pp. 143–148, 2023, doi: 10.21580/wjc.v6i2.17291.
- [32] W. Trisunaryanti, R. Shiba, M. Miura, M. Nomura, N. Nishiyama, and M. Matsukata, “Characterization and modification of Indonesian natural zeolites and their properties for hydrocracking of a paraffin,” *Sekiyu Gakkaishi (Journal Japan Pet. Institute)*, vol. 39, no. 1, pp. 20–25, 1996, doi: 10.1627/jpi1958.39.20.
- [33] N. Otandi, “Effect of Catalyst Concentration on Reaction Rate in Organic Synthesis in Kenya,” *J. Chem.*, vol. 3, no. 2, pp. 1–11, 2024, doi: 10.47672/jchem.2401.